SUPERSONIC FLOW PAST A SLENDER DELTA WING

- AN EXPERIMENTAL STUDY

J.L. Stollery and I.C. Richards
College of Aeronautics, Cranfield, Bedford, England

Abstract

A detailed survey of the flow around a delta wing with 70° of leading edge sweep has been performed at a Mach number of 2.5. Both leeside and windward surfaces have been studied over the incidence range $-5^{\circ} \leq \alpha \leq 50^{\circ}$. The measurements include upper and lower surface pressure distributions, schlieren photographs, vapour screen pictures and surface oil flow visualisation.

The results are compared with thin shock-layer theory. The agreement is generally good but the conjecture that the theory can be used to predict the occurrence of leading-edge separation needs further investigation.

1. Introduction

Although the supersonic flow over a delta wing has been the subject of extensive experimental and theoretical studies, some aspects of the flow remain unpredictable. In particular it is hard to define the type of leeside flow to be found when the windward side supports a detached shock wave. For a sharp subsonic leading edge the flow coming around the edge from the lower surface either separates and rolls up to form a spiral vortex as in the low speed flow, or expands through a Prandtl-Meyer fan to remain attached over the top surface. Stanbrook and Squire[1] found a rough empirical boundary between these two types of flow by plotting the change-over region on a graph of incidence normal to the leading edge versus the normal component of Mach number.

On the theoretical side Messiter's[2] thin shock layer concept has been extended and modified by many authors. The theory is now capable of describing (with considerable accuracy) the windward surface flow past slender and non-slender delta wings, supporting either attached or detached shock waves, at hypersonic or even modest supersonic speeds. Squire[3] has even used thin shock layer theory to suggest a connection between the windward and leeside flows (when the lower surface shock is detached) and hence to predict the onset of leading edge separation and the formation of spiral vortices over the top surface. Although this 'prediction' agreed reasonably well with the empirical Stanbrook-Squire boundary some more recent calculations by Hillier and Woods[4] have cast doubt on Squire's conjecture.

The aims of our investigation were to test some of the predictions and conjectures of thin shock layer theory by measuring the pressure distribution and flow field over a delta wing at a Mach number of 2.45. A very wide incidence range was covered and the tests were specifically designed to cut across the Stanbrook-Squire boundary. Deliberate attempts were made to minimise the effects of sting interference.

2. Apparatus

Dimensions and details of the models are given in Figure 1. Some earlier tests by Richards[5] had shown that filling in the base of a model with a 'telephone exchange' of pressure tubes could cause appreciable flow interference over the model. For this reason two models were made, one with spanwise tubes let into the top surface, the other with spanwise tubes in the lower surface. In each model the tubes were led away through a small diameter hollow sting. Two interchangeable stings were used, one straight, the other with a 25° dog-leg. With the normal quadrant incidence range of 30° the two stings enabled the model incidence range of $-50^{\circ} \leq \alpha \leq 50^{\circ}$ to be covered, with a 5° overlap (from 20° to 25°) to check whether the type of sting used had any effect.

The tests were made in the College of Aeronautics 9" x 9" continuous supersonic tunnel with a fixed single-sided nozzle liner. The test conditions were

$M_{\infty} = 2.5, \quad p_t = 3.5 \times 10^4 \, Nm^{-2}$ (0.36 atmospheres)

$Re_{\ell} = 4 \times 10^5, \quad$ Adiabatic Wall

The surface pressure tubes were drilled initially at 2mm from the leading edge. The nine static pressures were scanned sequentially by a pressure switch feeding a 0-10psia "Statham" transducer mounted external to the tunnel. The data were recorded using a "Dynamco" data logger and teletype.

Having covered the whole incidence range new holes were drilled successively nearer the model centre line and the outer holes plugged with beeswax.

A conventional single-pass schlieren was used with the knife edge parallel to the freestream direction.

For the vapour screen pictures some steam was injected just upstream of the nozzle throat. The flow was illuminated by a strong, thin, sheet of light and recorded on high speed film using a 35mm camera on full aperture for typically 30 seconds. Figure 2 shows the major features recorded and an actual vapour screen picture.

In the oil flow tests two techniques were used. The whole model was painted with a mixture of

titanium dioxide, gear oil and oleic acid. Exposure to the flow for 15 minutes gave a useful overall picture of the surface flow pattern. Subsequently the oil dot technique was used to obtain a simple, clear indication of the windward-side streamline directions.

3. Theory

The supersonic flow over a delta wing depends on the geometric variables of sweepback, thickness, incidence and leading edge radius plus the flow parameters of Mach number and Reynolds number. Fortunately this formidable list can be reduced to two dominant parameters by considering the Mach number component normal to the leading edge (M_n) and the flow inclination in this plane (α_n). These components are related to the free-stream conditions by

$$M_n = M_\infty(1 - \sin^2 \lambda \cos^2 \alpha)^{\frac{1}{2}} \qquad (1)$$

and

$$\alpha_n = \tan^{-1} \left\{ \frac{\tan \alpha}{\cos \lambda} \right\}$$

For a wing of given thickness angle (ψ) the shock detachment boundary can be constructed using the ordinary oblique shock charts or tables. Two such boundaries (for $\psi = 0^o$ and $\psi = 20^o$) are shown on Figure 3 together with the locus of test conditions for our model. Thus the model tested had subsonic leading edges at zero incidence and supported a detached shock over the whole incidence range. Also marked on Figure 3 is the shaded boundary suggested by Stanbrook and Squire from a survey of experimental data on a large number of delta wings which, though described as 'thin', covered the range $0^o < \psi \leq 30^o$. The boundary separates two types of lee-side flow. In type A the flow separates from the leading edge and the vortex sheet rolls up to form a spiral vortex. In type B the flow remains attached around the leading edge turning through a Prandtl-Meyer expansion to flow inward along the lee surface. An inboard shock may be needed to turn the flow streamwise and shock-boundary layer interaction may then modify the flow, (this is one area where the Reynolds number may be important). However, the distinction is clear based on the type of flow around the leading edge, A is separated, B is attached. In region C the shock is attached and the flow on the two surfaces should be sensibly independent. A similar picture, now with free-stream variables, M_∞ and α, is plotted in Figure 4. It can be seen that the test conditions have been chosen to cut through the Squire-Stanbrook boundary by changing incidence at a constant Mach number of 2.45.

Thin Shock-Layer Theory

Thin shock-layer theory is essentially a first order correction to simple Newtonian flow. Newtonian theory predicts that in the double limit $M_\infty \to \infty$, $\gamma \to 1$, the flow behind a given shock wave becomes infinitely dense so that the shock wave and body surface coalesce with all the captured air flowing within the infinitesimal surface layer. The initial deflection of any streamline meeting the shock must equal the local inclination of the shock and body (δ) at that point. The Newtonian value of pressure coefficient,

$$C_p = 2 \sin^2 \delta, \qquad (3)$$

is one of the very useful results from this inviscid theory.

The success of the Newtonian flow model, which assumes a zero thickness shock layer, naturally encourages the development of a modified and hopefully more accurate theory in which the shock layer is 'enlarged' from zero thickness to become just 'thin'. Messiter constructed such a theory which was subsequently developed and extended by a number of authors. The theory can now be used for a wide variety of shapes over a wide range of Mach number and incidence.

The numerical measure of the shock layer thickness used in thin shock-layer theory is the inverse density ratio across the basic shock wave,

$$\frac{\rho_\infty}{\rho_s} = \varepsilon = \frac{\gamma - 1}{\gamma + 1} + \frac{2}{(\gamma + 1)M_\infty^2 \sin^2 \bar{\alpha}} \qquad (4)$$

If the layer is very thin then $\bar{\alpha} \to \delta$. Writing the new theory as a correction to Newtonian and by considering known solutions and limiting cases the relevant expansions for the flow properties are

$$C_p = 2 \sin^2 \bar{\alpha} \{1 + \varepsilon P(y,z)\} + O(\varepsilon^2) \qquad (5)$$

$$\bar{u}/u_\infty = \cos \bar{\alpha} + \varepsilon u(y,z) + O(\varepsilon^2) \qquad (6)$$

$$\bar{v}/u_\infty = \varepsilon v(y,z) + O(\varepsilon^2) \qquad (7)$$

$$\bar{w}/u_\infty = \varepsilon^2 w(y,z) + O(\varepsilon^{3/2}) \qquad (8)$$

where y and z are scaled conical coordinates in the stretched system

$$x = \bar{x}, \qquad (9)$$

$$y = \bar{y}/\bar{x}.\varepsilon.\tan \bar{\alpha} \qquad (10)$$

and $$z = \bar{z}/\bar{x}.\varepsilon^{\frac{1}{2}}.\tan \bar{\alpha} \qquad (11)$$

Substitution of these relations in the continuity and momentum equations and the use of the boundary conditions at the shock and body surfaces yields a single integral equation relating the body and shock shapes. Knowing one shape the other can be calculated and the flow field and pressure distribution determined. For simple conical shapes (e.g., delta wings with diamond, roof-top or caret cross-sections) the solution can be found in terms of z/Ω, Ω and C where Ω is the reduced aspect ratio ($b/\varepsilon^{\frac{1}{2}}.\tan \bar{\alpha}$) and C is the reduced thickness parameter ($h/b\varepsilon^{\frac{1}{2}}$). Solutions have been found by many authors and a particularly clear discussion of the theory and the work undertaken up until 1970 is given by Roe[6]. It is important to note

although thin shock layer theory is powerful because of its simplicity and versatility (not to mention its success in predicting lower surface pressure distributions) it does represent a fairly drastic multilation of the full inviscid equations of motion

Originally the theory was intended for hypersonic conditions where the shock layer is indeed thin and the assumption that the 'basic shock' (i.e., that used to calculate ε) lay in the plane of the leading edges, was reasonable. At supersonic Mach numbers the shock position calculated from Messiter's theory can be well below the 'basic' position so Squire suggested a number of possible modifications. In his 'half-modified theory' Squire[7] relocates the basic shock half way between the plane of the leading edges and the maximum shock stand-off distance (i.e., that below the wing centre line) calculated by Messiter's theory. He then recalculates the pressure distribution etc. and new shock shape by re-applying thin shock layer theory but using the revised basic shock position. The process can be repeated again if necessary. In Squire's 'fully modified' theory the basic shock is placed at the maximum stand-off position rather than at the intermediate position described above. In this paper the theoretical predictions for the lower surface pressure distributions and the shock position at the model centreline have been made using the half-modified theory due to Squire.

When thin shock layer theory is used to predict the flow in the shock layer between a detached shock and the wing lower surface, two flow patterns are found. At low incidences the flow has three straight attachment lines (Fig. 5a), one of which is on the centre line. The outer pair lie very close to the leading edges and only move slowly inboard as the incidence is increased, hence little of the flow is 'spilt' around the leading edges.

However, some calculations by Shanbhag[8] suggested that at a particular 'critical' incidence the two outer attachement lines suddenly move to the centre to coalesce with the central one and give the flow pattern sketched in Figure 5b. In this pattern much more of the flow 'spills' around the leading edge and Squire[3] suggested that this change-over from Fig. 5a to Fig. 5b would be associated with the appearance of spiral vortices on the lee-surface, spring from leading edge separation. According to Shanbhag's analysis the change-over occurred at an incidence defined by a critical value of Ω, namely

$$\Omega = \Omega_{crit} = 0.5 + 1.2C. \qquad (12)$$

Comparison of this critical value with the empirical Stanbrook-Squire boundary looked promising. More recently Hillier and Woods have re-examined the work of Shanbhag and were unable to find the discontinuous behaviour of Ω and instead predict a smooth movement of the outer attachment lines towards the centre with no obvious definition of a critical point.

4. Results and Discussion

Flow Over The Windward Surface

The measured pressure distributions over the lower (compression) surface are plotted in conical co-ordinates and compared with half-modified thin shock layer theory in Figure 6. The way in which the measurements made at various chordwise stations collapse, confirms or denies the conical nature of the flow. The greatest deviation occurs at the highest incidence and at the rearmost station ($\bar{x}/\ell = 0.9$) and is presumably a trailing edge effect. The agreement with theory is very good even at incidences as low as 10^o where $\varepsilon > 1$, based on a shock lying in the leading edge plane. This is another indication that ε must be based on a shock position more closely related to the real shock position which, at the modest test conditions described here, lies well below the wing. With the 'half-way' position already mentioned the magnitude of ε is reduced and becomes more representative of the actual density ratio across the shock wave. The simple Newtonian values (of $2\sin^2 \alpha + \delta$) are shown at the left of the figure.

The trend of the shock wave angle with incidence (Fig. 7) is well predicted by the thin shock layer theory but the numerical values are about 3^o low. The simple oblique shock and conical shock values using the slope of the lower ridge line for the appropriate wedge or cone surface angle give no useful indication of the real shock position. The semi-empirical tangent-wedge relation

$$\frac{\theta}{\delta} = \frac{\gamma+1}{4} + \left\{ \left(\frac{\gamma+1}{4} \right)^2 + \frac{1}{(\beta\delta)^2} \right\}^{\frac{1}{2}} \text{ where } \beta^2 = M_\infty^2 - 1 \qquad (13)$$

is also shown and gives a fair indication of the actual shock angle.

The oil flow pictures at high incidence show the type of flow forecast in Figure 5b with a single central attachment line and the flow moving away from this line. At low incidence the oil flow pictures are more difficult to interpret. All the central flow is conically inward as shown in Figure 5a but the reattachment lines near the leading edge are difficult to see. However, the use of an oil dot technique confirmed their existence as shown in Figure 8.

Flow Over The Leeward Surface

The vapour screen pictures clearly show the start and development of the leading edge vortices and the locus of the enveloping shock wave. Separation from the leading edge forming a strong spiral vortex seems to occur for all positive incidences and at no time was an upper surface flow of the type shown in Figure 5a obtained. The pressure distributions (Figure 9) are also typical of vortex formation except close to the apex ($\bar{x}/\ell = 0.2$) where either the vortex has not had sufficient length to form or the measuring grid is too coarse to detect it. Superposition of the various spanwise pressure records shows that the lee-side flow is not conical but an outboard region of low pressure develops, typical of a zone beneath

a vortex core. The suction develops with incidence until about 80% of the absolute minimum is reached whereupon the spanwise distribution smooths out. The vapour screen pictures in fact show the vortex regions meeting on the centre-line at $\alpha = 25^{o}$ and overlapping for angles in excess of this value. The pressure distribution for $25^{o} \lesssim \alpha \lesssim 50^{o}$ is very roughly uniform over the entire upper surface with a value of 0.8 $C_{p(vac)}$.

The oil flow pictures again show leading edge separation and spiral vortex formation. As the incidence increases the tip regions under the vortices appear fully separated. This may well be due to the influence of the trailing edge.

Schlieren pictures show a dark line lying above the wing surface. The position of this line has been compared with the 'top' of the vortex as detected by the vapour screen technique. The good agreement shown in Figure 10 is obtained.

The most important finding from this investigation is the appearance of vortices on the lee-surface for all positive incidences. This is in some conflict with the Stanbrook-Squire 'boundary' which admittedly in practice is a somewhat large and nebulous region. The theoretical support for this boundary has now been shown by Hillier and Woods to be less definite since the discontinuity found by Shanbhag was due to the computional method employed rather than any real physical attribute of the governing equations. To check these new calculations Woods[9] some tests were run with the model inverted (i.e., the compression surface was now flat) and using the oil dot technique the inward movement of the outer pair of attachment lines was plotted. Figure 11 shows that Woods' calculations give a smooth continuous movement inward of the outer pair of attachment lines though the movement inward does accelerate as the incidence is raised. Woods used both the original and half-modified theories for his predictions. Figure 11 shows that our experimental data lie between the two but are closer to the unmodified theory.

Despite the dismissal of the theoretical boundary suggested by equation (12) there is obviously something physically attractive in trying to relate the windward and leeside flows. Since the edge is subsonic the flows cannot be independent. Moreover there cannot be much real flow around a sharp leading edge before separation occurs. The theoretical value of Ω for shock attachment is $\Omega = 2$. Woods has shown that $\Omega < 0.5$ the flow is entirely of the divergent type shown in Figure 5b. Hence somewhere in the region $2 < \Omega < 0.5$ the shock detaches, the three attachment line type of flow (Figure 5a) develops, flow begins to spill around the leading edge and the spillage increases with incidence (Ω decreasing) as the outer attachment lines converge on the central one. The question remains - is there a particular value of Ω in the range $2 < \Omega < 0.5$ which defines the appearance of leeside vortices?

From our last series of tests with a flat lower (compression) surface the leeside vortices first appeared around an incidence of 8^{o} (again measured relative to the flat surface). This corresponds to $\Omega \simeq 0.9$ using the half modified theory. However, any suggestion for a value of Ω crit must await the results of further investigation. In particular further analysis of the data collect by Stanbrook and Squire is needed in order to define the boundary more closely and to reconcile it with the results of this investigation.

6. Acknowledgements

This work was sponsored by the Procurement Executive, Ministry of Defence. The authors would like to thank Dr. L.C. Squire and the contract monitor Mr. P.L. Roe for many helpful discussions.

7. Nomenclature

b	max. semispan of wing.
C	reduced thickness parameter $(h/b\epsilon^{\frac{1}{2}})$
C_p	pressure coefficient
$C_{p(vac)}$	C_p in vaccuo = $-2/\gamma M_\infty^2$
h	max. thickness of wing
ℓ	length of the wing root chord
M_∞	freestream Mach number
M_n	Mach number component normal to the leading edge. Equation (1)
p	static pressure
p_t	total pressure
P	correction to the Newtonian pressure coefficient, see equation (5).
Re	Reynolds number
$\bar{u}$, $\bar{v}$, $\bar{w}$	physical velocity components
u, v, w	non dimensional velocity perturbations, see equations (6), (7) and (8)
$\bar{x}$, $\bar{y}$, $\bar{z}$	physical co-ordinates
x, y, z	transformed co-ordinates, see equations (9), (10), (11)
α	incidence of flat wing surface, see Figure 1
α_n	incidence measured normal to the leading edge {equation (2)}
$\bar{\alpha}$	incidence of the basic shock wave
β	$\sqrt{M_\infty^2 - 1}$
γ	ratio of specific heats
δ	local surface slope
ϵ	inverse density ratio across the basic shock, see equation (4)

θ	shock wave angle
λ	sweepback angle
ρ	density
ψ	thickness as measured by base angle see Figure 1
Ω	reduced aspect ratio, $(b/\varepsilon^{\frac{1}{2}} \tan \bar{\alpha})$

Suffices

crit	critical
vac	in vacuo
s	behind shock
∞	freestream

8. References

1. STANBROOK, A. and SQUIRE, L.C."Possible Types of Flow at Swept Leading Fdges", Aero. Quart. Vol. XV p.72 (1964).

2. MESSITER, A.F., "The Lift of Slender Delta Wings According to Newtonian Theory", AIAA J, Vol. 1, p. 794 (April 1963).

3. SQUIRE, L.C., "Flow Regimes over Delta Wings at Supersonic and Hypersonic Speeds", Aero. Quart., Vol XXVII, Part 1, pp. 1-14, (Feb, 1976).

4. HILLIER, R. and WOODS, B.A., "A Note on Detached-Shock Flows on Delta Wings in the Thin Shock Layer Approximation (to be published).

5. RICHARDS, I.C., "Pressure Measurements on the Suction Surface of a Flat Cone at M = 2.5.", College of Aeronautics Memo 7509, (1975).

6. ROE, P.L., "Thin Shock Layer Theory", AGARD Lecture Series No. 42, Vol. 1, Lecture 4, (1972).

7. SQUIRE, L.C., "Some Extensions of Thin Shock Layer Theory", Aero. Quart., Vol. XXV, p.1, (1974).

8. SHANBHAG, V.V., "Numerical Studies on Hypersonic Delta Wings with Detached Shock Waves", ARC Current Paper No. 1277, (1974).

9. WOODS, B.A., Private communication, (1976).

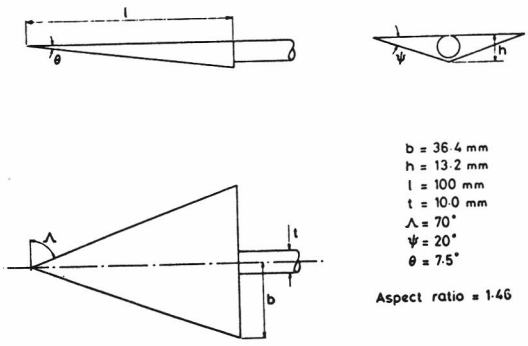

FIGURE 1. DIMENSIONS OF THE MODELS.

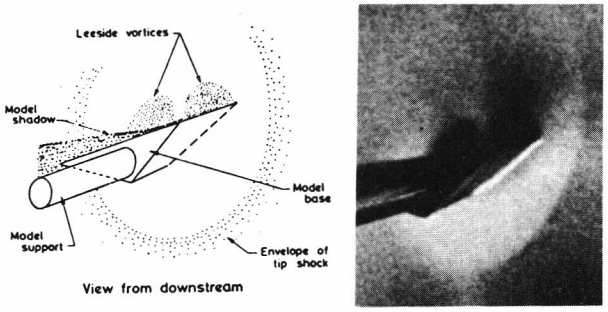

FIGURE 2. VAPOUR SCREEN PICTURE - SHOWING MAJOR FEATURES.

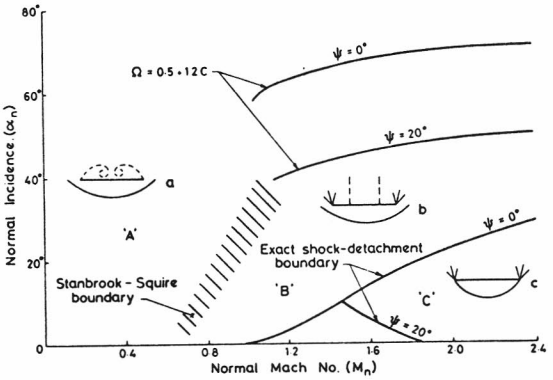

FIGURE 3. DIFFERENT FLOW REGIMES ON DELTA WINGS.

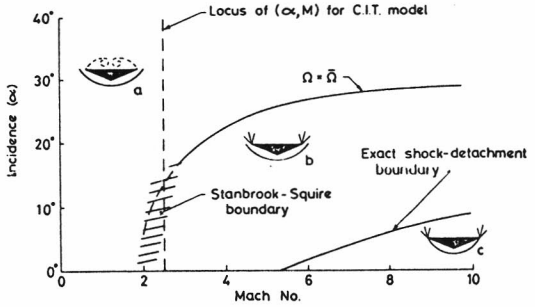

FIGURE 4. PREDICTIONS OF THE 'HALF-MODIFIED' THEORY FOR THE MODEL UNDER INVESTIGATION.

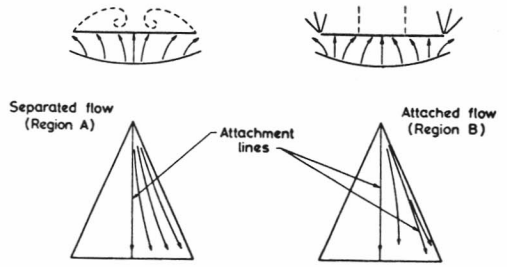

FIGURE 5. DIFFERENT FLOW PATTERNS IN REGIONS 'A' & 'B'

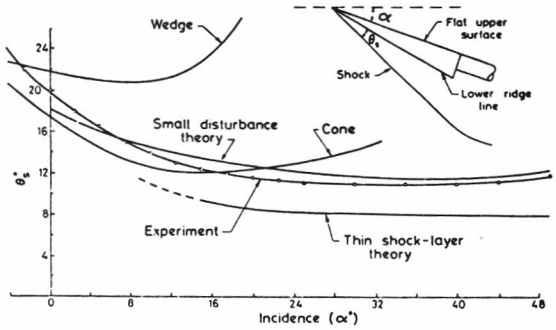

FIGURE 7. VARIATION OF SHOCK WAVE ANGLE WITH INCIDENCE

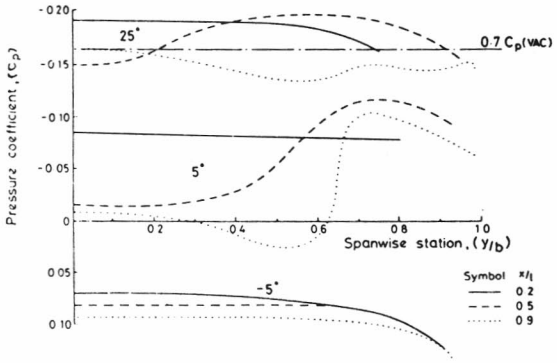

FIGURE 9. VARIATION OF PRESSURE WITH CORDWISE POSITION.

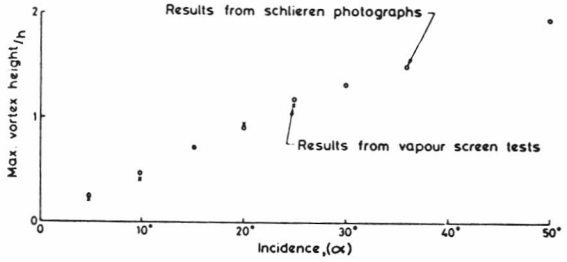

FIGURE 10. VARIATION OF VORTEX HEIGHT WITH INCIDENCE.

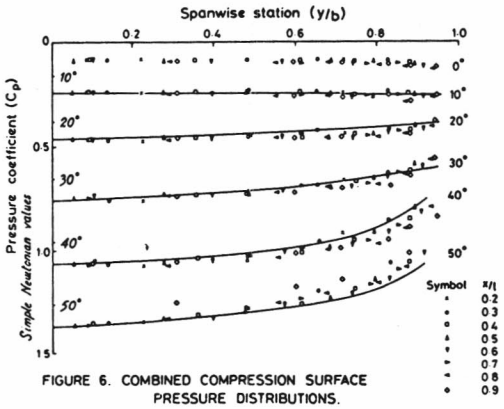

FIGURE 6. COMBINED COMPRESSION SURFACE PRESSURE DISTRIBUTIONS.

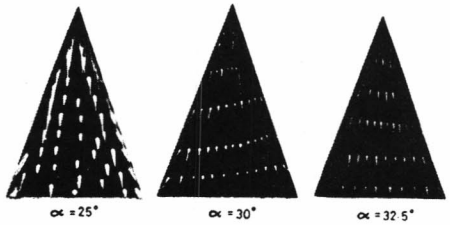

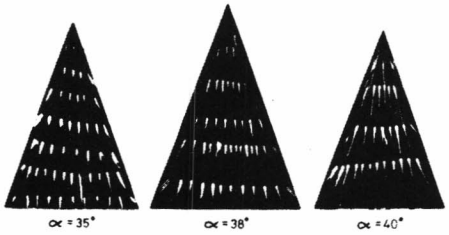

FIGURE 8. OIL FLOW ON FLAT COMPRESSION SURFACE.

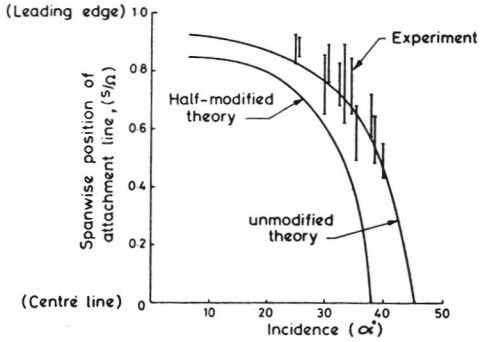

FIGURE 11. MOVEMENT OF COMPRESSION SURFACE ATTACHMENT LINES.